IJMF, Iranian Journal of Materials Forming, Vol. 1, No. 2, pp 52-62
Printed in The Islamic Republic of Iran, 2014

Fabrication of the Cu-Zn Multilayer and Cu-Zn Alloy by Accumulative Roll Bonding (ARB) with an Emphasis on the Wear Behavior

M. Reihanian[1*] M.M. Mahdavian[2] and L.Ghalandari[3]

[1]Department of Materials Science and Engineering, Faculty of Engineering, Shahid Chamran University of Ahvaz, Iran
[2]Department of Materials Science and Engineering, Ahvaz Branch, Islamic Azad University, Ahvaz, Iran
[3]Department of Materials Science and Engineering, Shiraz Branch, Islamic Azad University, Shiraz, Iran

Abstract: Accumulative roll bonding (ARB) was used to fabricate the Cu-Zn multilayer and Cu-Zn solid solution. A lamellar structure with the hardness of about 130 VHN was formed after eight ARB cycles. Following the suitable heat treatment, a solid solution with a uniform microstructure and hardness of about 57 VHN was produced. The dominant wear mechanism in the ARB processed multilayer was found to be delamination and spalling while in the heat-treated sample was adhesion. The weight loss of the ARBed multilayer was higher due to the occurrence of spalling and formation of the cracks and cavities during the ARB. On the other hand, the friction coefficient and its undulation were lower, which was contributed to the lubricating effect of Zn and the higher hardness of the ARB processed multilayer. In the heat-treated sample, the ability of plastic deformation and the adhesion between the contact surfaces causes the increase in the friction coefficient and its variation.

Keywords: Accumulative roll bonding, multilayer, solid solution, microstructure, wear

1. Introduction

Severe plastic deformation (SPD) is defined as a method of metal forming in which very large plastic strains are imposed into a bulk material without changing the overall dimensions of the sample [1]. The main objective of the SPD process is to produce an ultra-fine grained metal with excellent mechanical properties. Accumulative roll bonding (ARB) is one kind of SPD technique that consists of multiple cycles of stacking, rolling and cutting, so that large plastic strains are accumulated in the sheet metal without any significant change in the sheet dimensions [2]. Compared with the other SPD methods, ARB is simpler and cheaper and has the capability for commercialization. Thus far, ARB has been applied successfully to fabricate various ultra-fine grained sheet metals [3-6]. In recent years, ARB has also been introduced as a novel method to fabricate particulate metal matrix composites (MMCs) [7-11]. It has been shown that a uniform distribution of particles can be achieved after imposing a critical reduction [12, 13]. ARB has also been utilized to fabricate multi-component materials through processing a metallic multilayer such as Al/Mg [14], Al/Ni [15], Al/Cu [16], Cu/Ag [17], Al/Zn [18], Cu/ Nb [19], Cu/Ni [20] and Cu/Zn [21]. Cu/Zn/Al [22] and Al/Ni/Cu [23] are two examples for the tri-metallic systems processed through this method. During ARB of a multilayer, the hard layer necks and fractures due to the difference in the flow properties and concurrent deformation of dissimilar metals. After imposing a high number of ARB cycles, the fragments of the hard layer can uniformly distribute in the matrix and act as the reinforcement.

Although, the method of ARB has been utilized by many researchers to fabricate ultrafine-grained materials, MMCs and multi-component materials, the fabrication of a solid solution by ARB has attracted

Received by the editors October 7, 2014; Revised October 21, 2014 and Accepted October 22, 2014.
*Corresponding author (reihanian@scu.ac.ir)

little attentions [24]. In addition, the study of the wear behavior of composites made by ARB is limited only to that of the particulate ones [25-27] and no attempt has been made to investigate the wear behavior of a multi-component material. Accordingly, in this work, the Cu/Zn multilayer and Cu/Zn solid solution are fabricated by ARB with an emphasis on their wear behavior.

2. Materials and method

The materials utilized in this study were commercial pure Cu (99.9 wt. %) and Zn (98.86 wt. %) in the form of strips with the thickness of 1 mm. The strips were cut into 30 mm × 150 mm in size and annealed at 500 C for 60 min (for Cu) and at 150 C for 30 min (for Zn). The annealed strips were degreased by acetone and scratch brushed with a circular stainless steel brush with a wire diameter of 0.3 mm. The sheets were stacked with two Cu strips as the outer layers and one Zn strip as the inner layer. The primary sandwich was cold rolled through a 57% reduction in thickness. Then, it was conducted through a reduction of 50% in thickness and the process repeated up to eight cycles without lubrication. ARB experiments were conducted by a rolling machine with the capacity of 20 tons and rolling diameter of 170 mm. The rolling speed was set to 12 rpm.

After ARB, the multilayer was heated to 850 C for 3 hours and quenched in the cold water (0 C). Then, it was heated to 850 C for 3 hours and cooled slowly in the furnace. It is noted that the melting point of Cu and Zn is about 1100 C and 420 C, respectively. Regarding the initial dimensions of the Cu and Zn strips and using their densities, the composition (wt.%) of the Cu and Zn in the alloy is calculated as about 71% and 29%, respectively. By referring to the Cu-Zn phase diagram, this alloy will be a single solid solution with the melting point of about 900 C. Therefore, for the heat treated-temperature of 850 C, the alloy is in the solid state. The heat-treatment procedure was carried out in order to perfectly eliminate the effect of the mechanical processing, homogenize the microstructure and to form a solid solution alloy [24]. The pin-on-disk testing was used to determine the wear behavior of the specimens. The AISI 52100 steel (with the hardness of 63 HRC) and the sample were used as the pin and the disk, respectively. The sample was polished and cleaned with the ethanol before testing. The wear test was carried out without any lubricant under the normal atmosphere. The wear parameters were 0.5 m/s sliding velocity, 10 N load, and 1 km sliding distance.

The microstructure and the worn surface before and after the heat treatment were investigated by the field emission scanning electron microscope (FESEM) equipped with energy dispersive spectroscopy (EDS). In order to identify the phases, the x-ray diffraction (XRD) pattern of the composite was performed by a diffractometer, with a Cu Kα radiation and a step time of 58 s operating at 40 kV and 40 mA. The Vickers hardness was taken by applying a load of 30 kgf for 10 s on the surface of the strip surfaces.

3. Results and discussion

3.1. Microstructure

The XRD patterns after eight ARB cycles with and without heat treatment are presented in Fig.1. The symbols specified for every phase in the XRD pattern are presented in the legend of Fig.1. The pattern of the ARBed Cu/Zn multilayer indicates reflections due to the elements of Cu and Zn and a small peak of $CuZn_5$ intermetallic. The intermetallic may be formed due to the increase in the grain boundary and dislocation densities that accelerate the elemental diffusion at Cu and Zn interfaces. The formation of intermetallic phases has also been reported during ARB of other multilayers [14, 22, 28, 29]. After the

heat treatment, only the reflections of Cu are detected while its intensity increases and shifts to the lower angle side. This indicates that Zn and $CuZn_5$ are dissolved within the Cu lattice because sufficient activation energy is provided by thermal energy and a Cu/Zn solid solution is formed after the heat treatment. In the XRD pattern, the solid solution is specified by "Cu,Zn" and is denoted by the triangular sign.

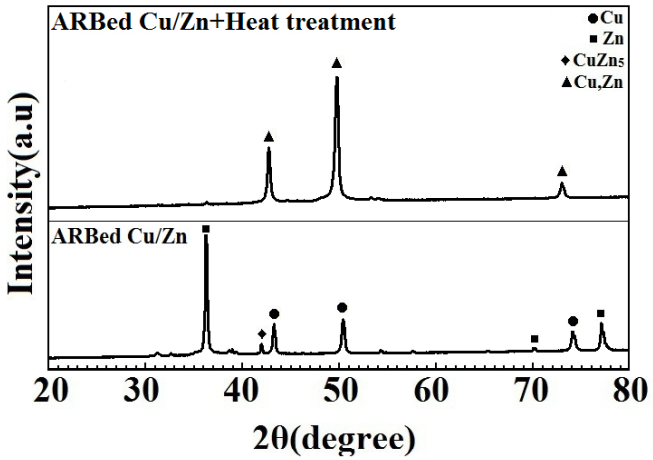

Fig. 1. The XRD pattern of the Cu/Zn multilayer after eight ARB cycles before (below) and after (above) the heat treatment.

SEM image and the corresponding elemental maps for Cu and Zn after eight ARB cycles are presented in Fig. 2. As can be seen, a lamellar structure is formed after eight cycles. The dark regions in the Zn layers may be the Kirkendall porosities that can be formed in diffusion couples when the diffusion rates of the two species are significantly different [30]. These porosities have previously been observed in the Zn layer during ARB of Cu/Zn/Al [22]. Kirkendall effect is a diffusional process that normally needs the thermal energy to overcome the activation energy for diffusion. ARB can decrease the activation energy for diffusion through increasing the lattice strain, dislocation density and grain boundary area as high-diffusivity paths. It seems that with the large 50% reduction at each ARB cycle, Kirkendall porosities must be closed, or at least elongated. However, SEM micrographs show that they are approximately spherical after ARB. These results indicate that Kirkendall porosities may be formed after exiting the multilayer from the roll gaps where enough time is provided for diffusion of the species. It is noted that, the formation of Kirkendall porosities under the dynamic or static conditions needs further investigation and is on the margin of the scope of this paper. The layer thickness decreases during ARB through an equation of the form $(t_0/2^n)$ where t_0 is the initial layer thickness and n is the number of cycles. Therefore, for a 1 mm layer thickness, the thickness of the layer (or available distance for diffusion of species) will reduce to about 4 μm after eight ARB cycles.

Figure 2 also reveals several microcracks at the interface of Cu and Zn that can be attributed to the formation of the $CuZn_5$ intermetallic. The volume changes during intermetallic formation and the expansion mismatch between the intermetallic and adjacent layers can create cracks between the layers [31, 32]. SEM/elemental mapping of ARBed Cu/Zn composite after the heat-treatment is presented in Fig. 3. It is observed that the lamellar structure no longer exists and all elements are distributed uniformly in the microstructure. These results together with the XRD patterns indicate that the heat treatment provides sufficient times and temperature to obtain a solid solution from the ARBed Cu/Zn multilayer.

However, the detrimental effect of the annealing treatment (grain growth, etc.) should be considered when a solid solution is formed. It is noticed that the effect of the ARB cycle and the heat treatment conditions on the solid solution formation is not the goal of the present study and needs further investigations.

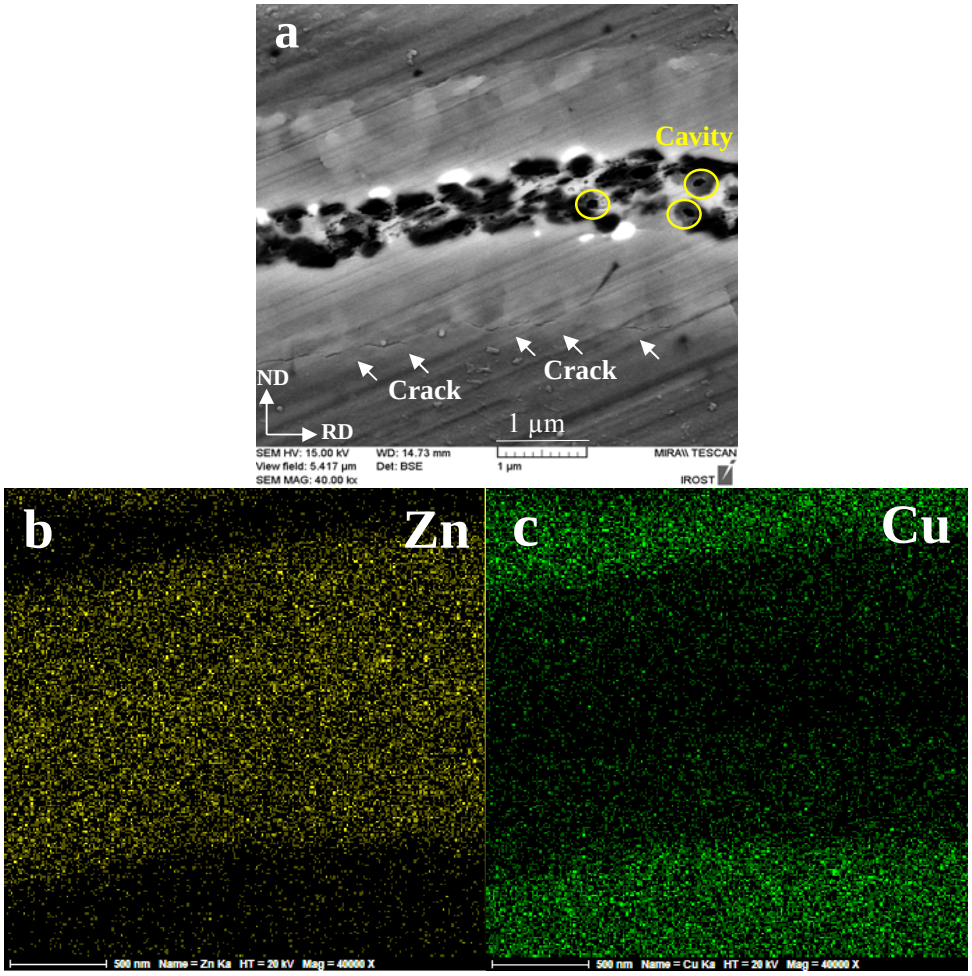

Fig. 2. (a) SEM image of Cu/Zn multilayer after eight ARB cycles and the corresponding elemental maps for (b) Zn and (c) Cu distribution.

3.2. Morphology of the worn surfaces

The appearance of the worn surfaces for the ARBed Cu/Zn sample after eight ARB cycles is shown in Fig. 4. The worn surfaces show several morphological features such as pits, spalls, cracks and flakes at low and high magnifications, which are the most important aspects of the delamination [33]. Delamination is caused by the repeated sliding of the asperities across the surface of the solids in the relative motion. The local plasticity during wear has a cyclic component. The unidirectional shearing of the metal surface nucleates the voids beneath the surface that extend and link up to form a subsurface crack parallel to the surface. When the crack becomes sufficiently large, it breaks out to give the flake-like wear fragments and leaves the so-called anion peeling morphology on the worn surface. The nucleation and propagation of the subsurface cracks can also result in several surface cracks near the delaminated flakes (as marked in Fig. 4).

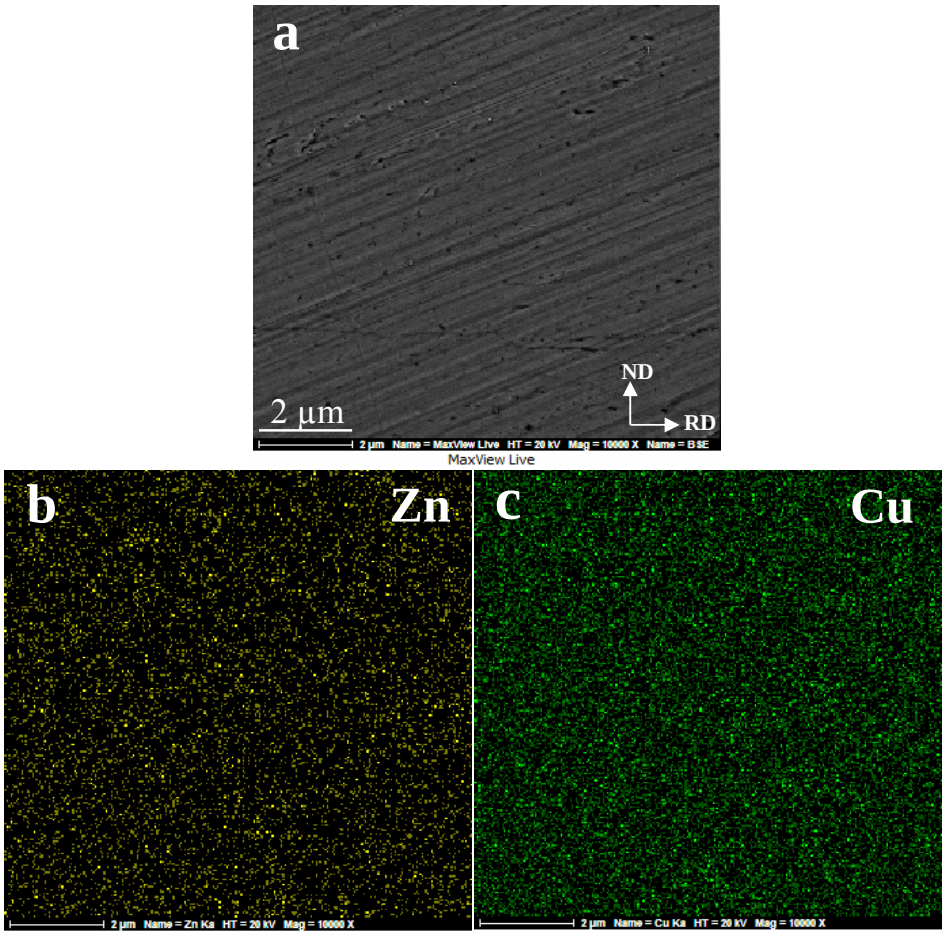

Fig. 3. (a) SEM image of ARBed Cu/Zn multilayer after the heat treatment and the corresponding elemental maps for (b) Zn and (c) Cu distribution.

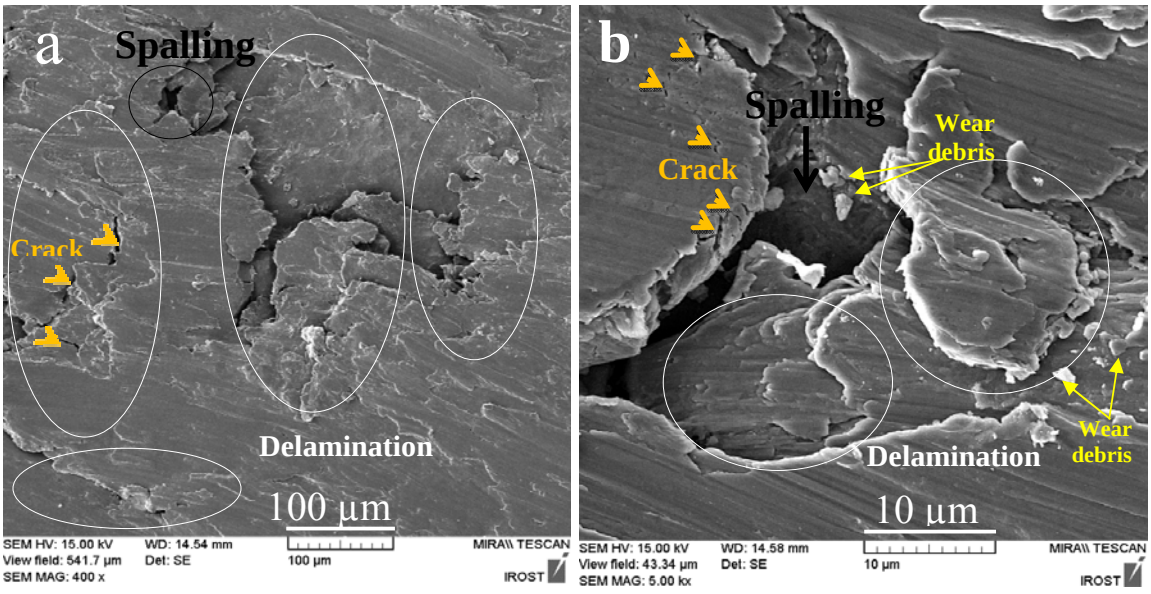

Fig. 4. The worn surface morphology (after wear) of the Cu/Zn multilayer at (a) low and (b) high magnification.

In the ARBed Cu/Zn multilayer, several factors can support and promote the origin of delamination. The microstructure of Cu/Zn represents a lamellar structure, which is preserved after eight cycles (see Fig. 2). As the ARB proceeds, the layer thickness decreases and the number of interfaces increases. For a given penetration depth of wear, the number of layer interfaces that are located in the wear volume increases with increasing the number of cycles. Since, the interfaces are good locations for crack nucleation, the probability of crack formation increases as the number of ARB cycles increases. This result is consistent with that of Al/Al_2O_3 composite at large number of ARB cycles [27]. Formation of the intermetallic and Kirkendall porosities during ARB (Fig. 2), are additional factors that promote the crack formation and delamination.

Further inspection of the worn surface of the ARBed Cu/Zn multilayer reveals another surface morphology, the so-called spalling, that appear as a deep hollow. Spalling takes place when the subsurface cracks propagate in the direction of the flow lines in the deformation zone [27]. Therefore, spalling can be another mechanism for the removal of material in ARBed Cu/Zn multilayer. It is noted that both delamination and adhesion are regarded as the two responsible mechanisms for the plasticity-dominated wear [34]. The worn surface of the ARBed Cu/Zn multilayer after the heat treatment (Fig. 5) illustrates the trace of severe plastic deformation as well as furrows and ridges along the sliding direction because of squashing and plowing by the counterface. These traces indicate that the adhesion can be the dominant wear mechanism. Nonetheless, the presence of scratches in the worn surface indicates that the wear can also be progressed to some extent by an abrasive mechanism.

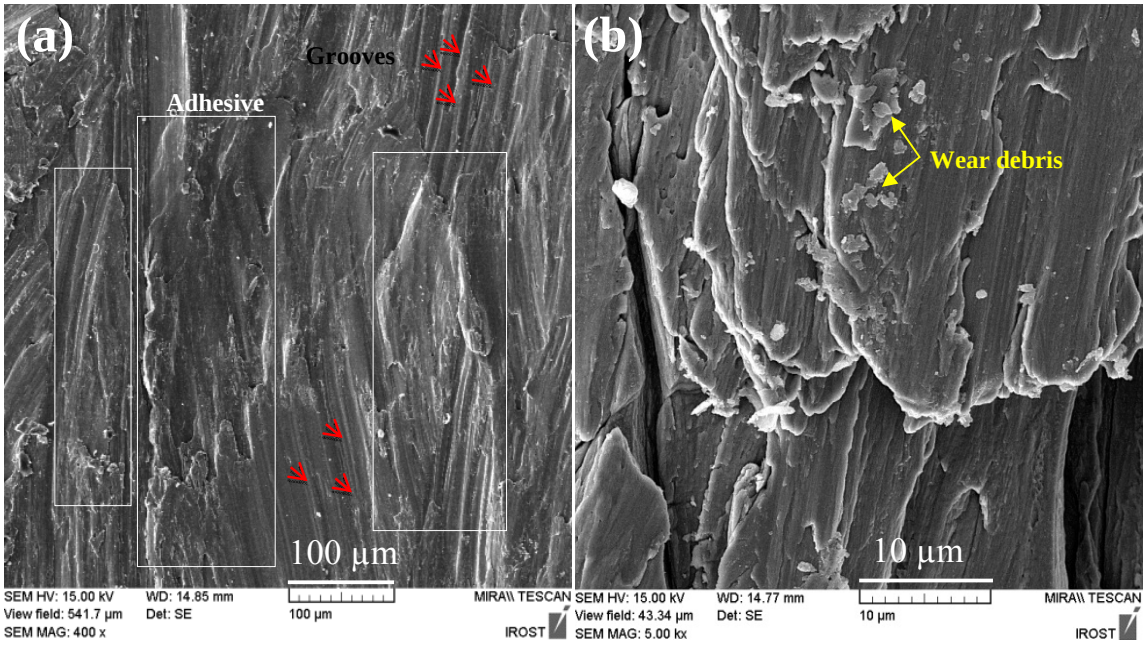

Fig. 5. The worn surface morphology (after wear) of the Cu/Zn solid solution at (a) low and (b) high magnification

3.3. Wear rate and friction coefficient

According to the literature [35], several factors can affect the wear behavior of the SPD processed materials. Some of them improve the wear resistance and the others reduce it. Grain refinement and the increase in hardness are the factors that improve the wear resistance of the SPD processed materials. In contrast, the decrease in ductility and work hardening capability are reported to be the main factors that reduce the wear resistance of these materials.

Figure 6 shows the results of the wear resistance expressed as the weight loss for ARBed Cu/Zn before and after the heat treatment. It is noteworthy that the material after the heat treatment can be considered as a non-processed material because the heat treatment can perfectly eliminate the effect of the mechanical processing and homogenize the microstructure. Results show that the weight loss of the ARBed Cu/Zn multilayer is somewhat higher than that of the heat-treated sample in spite of its higher hardness (about 130 VHN). The wear behavior of Cu/Zn multilayer reveals a discrepancy with the Archard equation [36] in which the wear rate is inversely proportional to the hardness or strength of the material. Therefore, other material parameters may influence the wear behavior of the material as well as hardness. The decrease in the wear resistance of the Cu/Zn multilayer after ARB is consistent with the results of the Al and Al alloys processed by ARB [37-39]. This behavior is attributed to the low work hardening capability of the material after ARB and to the subsurface microstructure and its evolution during the wear process [39].

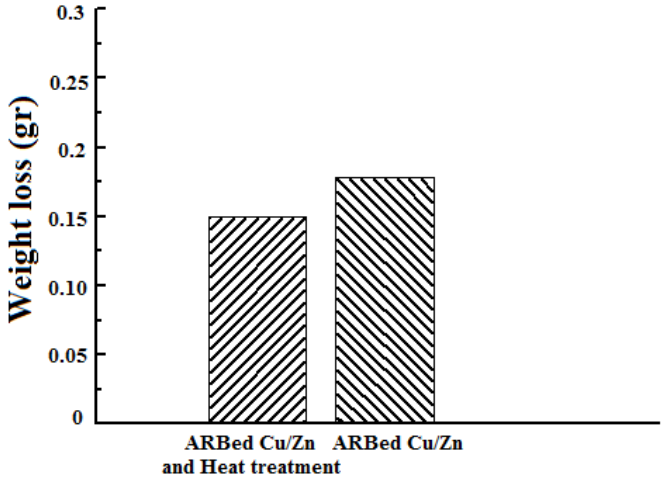

Fig. 6. The weight loss of the ARBed Cu/Zn multilayer before and after the heat treatment

Due to the complex nature of the wear behavior of SPD processed materials [40], modeling the mechanism of the wear is somewhat difficult. The higher wear rate of the ARBed Cu/Zn multilayer can be explained by the model proposed by Kazemi Talachi et al [39]. According to the model, the temperature rise at the contact surfaces changes the ultrafine-grained structure beneath the surface into a coarse-grained one due to the recrystallization and grain growth. The strain incompatibility between the two-grain structures leads to the delamination of the coarse-grained structure. In addition, in the Cu/Zn multilayer, the formation of the microcracks and porosities can also decrease the bond strength and provide suitable sites for delamination. These effects are more realistic than the proposed model because they are observed on the microstructure. Another responsible mechanism that can be attributed to the higher rate of wear is spalling [27].

Figure 7 shows the friction coefficient of the ARBed Cu/Zn multilayer before and after the heat treatment. In general, the coefficient of friction and its amplitude variation for the ARBed Cu/Zn multilayer are lower. For the initial 200 m sliding distance, the friction coefficient of the ARBed Cu/Zn multilayer displays little fluctuation while it shows higher variation for the remaining 800 m distance. This may be attributed to the increase of fracturing and delamination at relatively large sliding distances. The lower friction coefficient of the ARBed Cu/Zn multilayer may be correlated to the lamellar structure of the multilayer in which the Zn can act as a solid lubricant due to its hexagonal closed packed (HCP) structure. The lubricating effect of Zn is similar to Ag (a soft noble metal) [41], carbon nanotube [42, 43] and rare

earth elements [44]. The lower friction coefficient of the ARBed Cu/Zn multilayer can also be due to the increase of the hardness (about 130 VHN) during ARB because of the grain refinement. On the other hand, the higher value of friction coefficient as well as its variation for the heat-treated sample can be associated with the adhesion wear, which is the dominant wear mechanism under these conditions. The lower value of the hardness measured for the heat-treated sample (about 57 VHN) and its capability for plastic deformation, result in the higher real area of contact and adhesion. The interactions of asperities on the surfaces affect the coefficient of friction, which is varying in the specific range during the sliding.

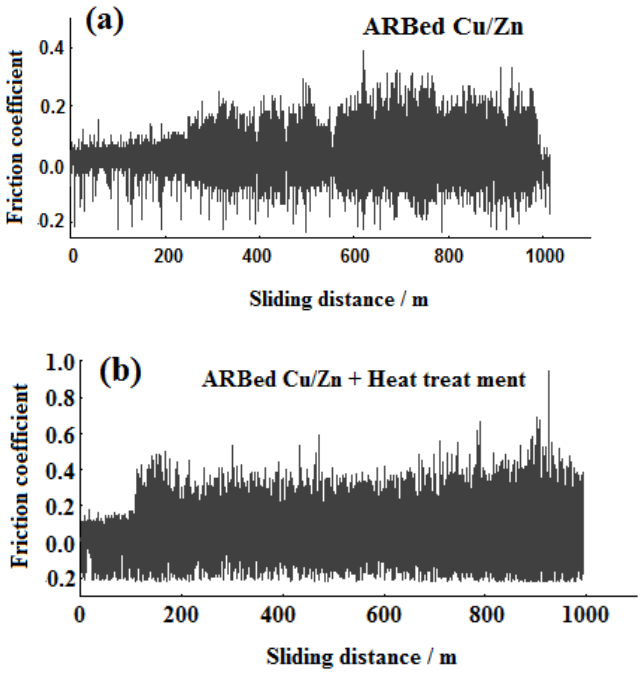

Fig. 7. Variation in the friction coefficient with sliding distance for ARBed Cu/Zn multilayer (a) before and (b) after the heat treatment

4. Conclusion

The Cu/Zn multilayer was processed by ARB up to eight cycles. The microstructure and wear behavior were investigated before and after the heat treatment. The following results are obtained:

1. A lamellar microstructure is obtained after imposing eight ARB cycles. The intermetallic and microcracks are formed at layer interfaces. The cavities are also created in the Zn layer as well. After the heat-treatment, a copper solid solution with a uniform microstructure is formed.
2. Delamination and spalling are the dominant wear mechanisms in the ARBed Cu/Zn multilayer. The laminated structure, microcracks and porosities promote the origin of cracking. The worn surface after the heat treatment illustrates that adhesive wear is the dominant mechanism.
3. The weight loss of the ARBed Cu/Zn multilayer is higher. The low work hardening capability, subsurface microstructure, microcracks and porosities are the main factors that reduce the wear resistance of the multilayer.
4. The friction coefficient and its undulation of the ARB processed multilayer are lower due to the self-lubricating effect of Zn and higher hardness value. The low hardness value and the capability for plastic deformation cause the adhering between the contact surfaces and variation of friction coefficient in the heat-treated sample.

5. References

[1] R.Z. Valiev and T.G. Langdon, Principles of equal-channel angular pressing as a processing tool for grain refinement, *Progress in Materials Science*, 51 (2006) 881-981.

[2] Y. Saito, H. Utsunomiya, N. Tsuji and T. Sakai, Novel ultra-high straining process for bulk materials—development of the accumulative roll-bonding (ARB) process, *Acta Materialia*, 47 (1999) 579-583.

[3] B.L. Li, N. Tsuji and N. Kamikawa, Microstructure homogeneity in various metallic materials heavily deformed by accumulative roll-bonding, *Materials Science and Engineering: A*, 423 (2006) 331-342.

[4] J.L. Milner, F. Abu-Farha, C. Bunget, T. Kurfess and V.H. Hammond, Grain refinement and mechanical properties of CP-Ti processed by warm accumulative roll bonding, *Materials Science and Engineering: A*, 561 (2013) 109-117.

[5] A.L.M. Costa, A.C.C. Reis, L. Kestens and M.S. Andrade, Ultra grain refinement and hardening of IF-steel during accumulative roll-bonding, *Materials Science and Engineering: A*, 406 (2005) 279-285.

[6] N. Tsuji, T. Iwata, M. Sato, S. Fujimoto and Y. Minamino, Aging behavior of ultrafine grained Al–2wt%Cu alloy severely deformed by accumulative roll bonding, *Science and Technology of Advanced Materials*, 5 (2004) 173-180.

[7] M. Alizadeh and M.H. Paydar, Fabrication of nanostructure Al/SiCP composite by accumulative roll-bonding (ARB) process, *Journal of Alloys and Compounds*, 492 (2010) 231-235.

[8] R. Jamaati and M.R. Toroghinejad, Application of ARB process for manufacturing high-strength, finely dispersed and highly uniform Cu/Al2O3 composite, *Materials Science and Engineering: A*, 527 (2010) 7430-7435.

[9] M. Rezayat, A. Akbarzadeh and A. Owhadi, Fabrication of High-Strength Al/SiC p Nanocomposite Sheets by Accumulative Roll Bonding, *Metallurgical and Materials Transaction A*, 43 (2012) 2085-2093.

[10] A. Yazdani and E. Salahinejad, Evolution of reinforcement distribution in Al–B4C composites during accumulative roll bonding, *Materials & Design*, 32 (2011) 3137-3142.

[11] M. Reihanian, F.K. Hadadian and M.H. Paydar, Fabrication of Al–2vol% Al2O3/SiC hybrid composite via accumulative roll bonding (ARB): An investigation of the microstructure and mechanical properties, *Materials Science and Engineering: A*, 607 (2014) 188-196.

[12] M. Reihanian, E. Bagherpour and M.H. Paydar, Particle distribution in metal matrix composites fabricated by accumulative roll bonding, *Materials Science and Technology*, 28 (2012) 103-108.

[13] M. Reihanian, E. Bagherpour and M.H. Paydar, On the achievement of uniform particle distribution in metal matrix composites fabricated by accumulative roll bonding, *Materials Letters*, 91 (2013) 59-62.

[14] K. Wu, H. Chang, E. Maawad, W.M. Gan, H.G. Brokmeier and M.Y. Zheng, Microstructure and mechanical properties of the Mg/Al laminated composite fabricated by accumulative roll bonding (ARB), *Materials Science and Engineering: A*, 527 (2010) 3073-3078.

[15] A. Mozaffari, H. Danesh Manesh and K. Janghorban, Evaluation of mechanical properties and structure of multilayered Al/Ni composites produced by accumulative roll bonding (ARB) process, *Journal of Alloys and Compounds*, 489 (2010) 103-109.

[16] M. Eizadjou, A. Kazemi Talachi, H. Danesh Manesh, H. Shakur Shahabi and K. Janghorban, Investigation of structure and mechanical properties of multi-layered Al/Cu composite produced by accumulative roll bonding (ARB) process, *Composites Science and Technology*, 68 (2008) 2003-2009.

[17] L. Ghalandari and M.M. Moshksar, High-strength and high-conductive Cu/Ag multilayer produced by ARB, *Journal of Alloys and Compounds*, 506 (2010) 172-178.

[18] R.N. Dehsorkhi, F. Qods and M. Tajally, Investigation on microstructure and mechanical properties of Al–Zn composite during accumulative roll bonding (ARB) process, *Materials Science and Engineering: A*, 530 (2011) 63-72.

[19] J. Wang, K. Kang, R.F. Zhang, S.J. Zheng, I.J. Beyerlein and N.A. Mara, Structure and property of interfaces in ARB Cu/Nb laminated composites, *JOM*, 64 (2012) 1208-1217.

[20] M. Tayyebi & B. Eghbali, Study on the microstructure and mechanical properties of multilayer Cu/Ni composite processed by accumulative roll bonding, *Materials Science and Engineering: A*, 559 (2013) 759-764.

[21] L. Ghalandari, M.M. Mahdavian and M. Reihanian, Microstructure evolution and mechanical properties of Cu/Zn multilayer processed by accumulative roll bonding (ARB), *Materials Science and Engineering: A*, 593 (2014) 145-152.

[22] M.M. Mahdavian, L. Ghalandari, M. Reihanian, Accumulative roll bonding of multilayered Cu/Zn/Al: An evaluation of microstructure and mechanical properties, *Materials Science and Engineering: A*, 579 (2013) 99-107.

[23] A. Shabani, M.R. Toroghinejad, A. Shafyei, Fabrication of Al/Ni/Cu composite by accumulative roll bonding and electroplating processes and investigation of its microstructure and mechanical properties, *Materials Science and Engineering: A*, 558 (2012) 386-393.

[24] M. Reihanian, M.M. Mahdavian, L. Ghalandari, A. Obeidavi, Formation of a Solid Solution Through Accumulative Roll Bonding (ARB) and Post-Heat Treatment of Multilayered Cu/Zn/Al, *Iranian Journal of Materials Forming*, 1 (2014) 24-31.

[25] C.Y. Liu, Q. Wang, Y.Z. Jia, B. Zhang, R. Jing, M.Z. Ma, Q. Jing and R.P. Liu, Evaluation of mechanical properties of 1060-Al reinforced with WC particles via warm accumulative roll bonding process, *Materials & Design*, 43 (2013) 367-372.

[26] E. Darmiani, I. Danaee, M.A. Golozar, M.R. Toroghinejad, A. Ashrafi and A. Ahmadi, Reciprocating wear resistance of Al–SiC nano-composite fabricated by accumulative roll bonding process, *Materials & Design*, 50 (2013) 497-502.

[27] R. Jamaati, M. Naseri and M.R. Toroghinejad, Wear behavior of nanostructured Al/Al2O3 composite fabricated via accumulative roll bonding (ARB) process, *Materials & Design*, 59 (2014) 540-549.

[28] H. Chang, M.Y. Zheng, C. Xu, G.D. Fan, H.G. Brokmeier and K. Wu, Microstructure and mechanical properties of the Mg/Al multilayer fabricated by accumulative roll bonding (ARB) at ambient temperature, *Materials Science and Engineering*: A, 543 (2012) 249-256.

[29] S.J. Yoo, S.H. Han and W.J. Kim, Magnesium matrix composites fabricated by using accumulative roll bonding of magnesium sheets coated with carbon-nanotube-containing aluminum powders, *Scripta Materialia*, 67 (2012) 129-132.

[30] I.D. Choi, D.K. Matlock and D.L. Olson, An analysis of diffusion-induced porosity in Cu-Ni laminate composites, *Materials Science and Engineering: A*, 124 (1990) L15-L18.

[31] A. Mozaffari, M. Hosseini and H.D. Manesh, Al/Ni metal intermetallic composite produced by accumulative roll bonding and reaction annealing, *Journal of Alloys and Compounds*, 509 (2011) 9938-9945.

[32] M. Danaie, C. Mauer, D. Mitlin and J. Huot, Hydrogen storage in bulk Mg–Ti and Mg–stainless steel multilayer composites synthesized via accumulative roll-bonding (ARB), *International Journal of Hydrogen Energy*, 36 (2011) 3022-3036.

[33] K.H.Z. Gahr, Microstructure and Wear of Materials, 1st ed. Netherland: Elsevier Science, (1987).

[34] S.C. Lim and M.F. Ashby, Overview no. 55 wear-mechanism maps, *Acta Metallurgica*, 35 (1987) 1-24.

[35] N. Gao, C. Wang, R.K. Wood and T. Langdon, Tribological properties of ultrafine-grained materials processed by severe plastic deformation, *Journal of Materials Science*, 47 (2012) 4779-4797.

[36] J.F. Archard, Contact and Rubbing of Flat Surfaces, *Journal of Applied Physics*, 24 (1953) 981-988.

[37] M.E. A. Kazemi Talachi, H. Danesh Manesh and K. Janghorban, Wear properties of 1100 Al alloy produced by accumulative roll bonding, *International Journal of Modern Physics B*, 22 (2008).

[38] M. Eizadjou, H.D. Manesh and K. Janghorban, Microstructure and mechanical properties of ultra-fine grains (UFGs) aluminum strips produced by ARB process, *Journal of Alloys and Compounds*, 474 (2009) 406-415.

[39] A.K. Talachi, M. Eizadjou, H.D. Manesh and K. Janghorban, Wear characteristics of severely deformed aluminum sheets by accumulative roll bonding (ARB) process, *Materials Characterization*, 62 (2011) 12-21.

[40] C. Wang, N. Gao, R.K. Wood and T. Langdon, Wear behavior of an aluminum alloy processed by equal-channel angular pressing, *Journal of Materials Science*, 46 (2011) 123-130.

[41] X. Shi, Z. Xu, M. Wang, W. Zhai, J. Yao, S. Song, A. Qamar ud Din and Q. Zhang, Tribological behavior of TiAl matrix self-lubricating composites containing silver from 25 to 8000;°C, *Wear*, 303 (2013) 486-494.

[42] M.M.H. Bastwros, A.M.K. Esawi and A. Wifi, Friction and wear behavior of Al–CNT composites, *Wear*, 307 (2013) 164-173.

[43] A.M. Al-Qutub, A. Khalil, N. Saheb and A.S. Hakeem, Wear and friction behavior of Al6061 alloy reinforced with carbon nanotubes, *Wear*, 297 (2013) 752-761.

[44] A. Zafari, H.M. Ghasemi and R. Mahmudi, Effect of rare earth elements addition on the tribological behavior of AZ91D magnesium alloy at elevated temperatures, *Wear*, 303 (2013) 98-108.